

Mutations in the gene encoding SLURP-1 in Mal de Meleda

Judith Fischer^{1,*}, Bakar Bouadjar², Roland Heilig³, Marcel Huber⁴, Caroline Lefèvre¹, Florence Jobard¹, Françoise Macari⁴, Ana Bakija-Konsuo⁵, Farid Ait-Belkacem⁶, Jean Weissenbach³, Mark Lathrop¹, Daniel Hohl⁴ and Jean-François Prud'homme⁷

¹Centre National de Génotypage, 91057 Evry, France, ²Department of Dermatology CHU of Bab-El-Oued, Algiers, Algeria, ³Genoscope, CNS, 91057 Evry, France, ⁴Dermatogenetic Unit and Laboratory for Cutaneous Biology, Department of Dermatology, CHUV-DHURDV, 1011 Lausanne, Switzerland, ⁵Department of Dermatology, Dubrovnik General Hospital, Dubrovnik, Croatia, ⁶Department of Dermatology, Mustapha Hospital, Algiers, Algeria and ⁷Généthon, 91002 Evry, France

Received 21 December 2000; Revised and Accepted 12 February 2001

Mal de Meleda (MDM) is a rare autosomal recessive skin disorder, characterized by transgressive palmo-plantar keratoderma (PPK), keratotic skin lesions, perioral erythema, brachydactyly and nail abnormalities. We report the refinement of our previously described interval of MDM on chromosome 8qter, and the identification of mutations in affected individuals in the *ARS* (component B) gene, encoding a protein named SLURP-1, for secreted Ly-6/uPAR related protein 1. This protein is a member of the Ly-6/uPAR superfamily, in which most members have been localized in a cluster on chromosome 8q24.3. The amino acid composition of SLURP-1 is homologous to that of toxins such as frog cytotoxin and snake venom neurotoxins and cardiotoxins. Three different homozygous mutations (a deletion, a nonsense and a splice site mutation) were detected in 19 families of Algerian and Croatian origin, suggesting founder effects. Moreover, one of the common haplotypes presenting the same mutation was shared by families from both populations. Secreted and receptor proteins of the Ly-6/uPAR superfamily have been implicated in transmembrane signal transduction, cell activation and cell adhesion. This is the first instance of a secreted protein being involved in a PPK.

INTRODUCTION

The hereditary palmoplantar keratodermas (PPKs) are a heterogeneous group of skin diseases characterized by hyperkeratosis on the palms and soles with or without associated ectodermal or non-ectodermal features (1). In addition to defects in various structural proteins such as keratin intermediate filaments and loricrin, the major precursor protein of the cornified cell envelope, mutations of molecules involved in filament anchorage (plakoglobin, desmoplakin), cellular adhesion (desmoglein 1, plakophilin), formation of gap-junctions (connexins 26, 30

and 31) or proteolysis (cathepsin C) cause diverse variants of PPKs (1–3).

Mal de Meleda (MDM, MIM 248300) is a rare autosomal recessive PPK, characterized by keratotic skin lesions, particularly over the joints, perioral erythema, brachydactyly and nail abnormalities. Associated hyperhidrosis and superinfection frequently cause malodorous maceration. The progressive lesions can lead to severe functional handicap with reduced mobility of hands and feet including spontaneous amputation of digits.

We previously reported the localization of the MDM gene to chromosome 8qter by linkage analysis in two large consanguineous families (families 1 and 2), within an interval of at least 3 cM, but without definition of the telomeric limit (4). We refined this interval using a combination of homozygosity mapping and linkage disequilibrium analysis in 19 families. Mutation analysis of candidate genes in the interval revealed three different homozygous mutations in the *ARS* (component B) gene, encoding SLURP-1 (secreted Ly-6/uPAR related protein 1) (5) in these families. Secreted and receptor proteins of the Ly-6/uPAR superfamily have been implicated in transmembrane signal transduction (5), cell activation and cell adhesion (6).

RESULTS

Clinical features and patient origins

We studied 12 kindreds of Algerian origin and 7 kindreds from Croatia, including Meleda island (Mljet, which was formerly a leper colony), with a total of 41 patients and 104 unaffected family members. Three of these families have been previously described (families 1, 2 and 5; Fig. 1). Affected subjects presented typical symptoms of MDM, with the exception of three patients from two Algerian families (kindreds 7 and 10), who presented a phenotype with unusual presence of lesions in the inguinal area of the body and were therefore initially diagnosed as affected by a recessive form of progressive and symmetric erythrokeratoderma (PSEK, MIM 602036). Fourteen families were known to be consanguineous (13 from first

*To whom correspondence should be addressed. Tel.: +33 1 60 87 83 57; Fax: +33 1 60 87 83 83; Email: fischer@cng.fr

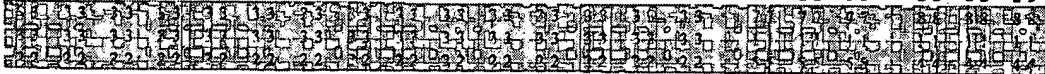
Patient	1.9	1.11	1.6	2.12	3.19	6.12	7.10	9.5	10.10	11.4	12.9	14.3	16.3	17.3	18.15	4.17	5.9	8.10	13.3	15.6	19.3
Origin	A	A	A	A	A	A	A	A	A	A	A	C	C	C	C	A	A	A	C	C	C
Marker																					
D8S1717	3 6	6 11	9 9	3 9	9 9	9 9	3 3	6 6	3 3	9 9	6 6	1 8	3 9	3 9	9 9	9 4	12 12	11 11	3 3	3 3	3 3
D8S1704	5 2	2 3	5 3	3 3	3 3	3 3	5 5	2 2	3 5	3 3	2 2	1 3	1 3	5 3	3 3	3 2	1 1	2 2	1 1	1 1	1 4
CNG001	7 3	3 4	4 5	11 5	7 7	5 5	2 2	3 3	5 2	5 5	3 3	4 6	4 6	1 5	6 6	2 5	6 6	4 4	4 4	4 4	4 8
D8S1727	3 4	- -	3 3	3 3	3 3	3 3	6 6	4 4	6 6	3 3	4 4	- -	- -	- -	- -	8 8	3 3	- -	8 8	8 8	8 8
CNG002	4 2	2 1	2 2	2 2	4 4	2 2	2 2	2 2	2 2	2 2	2 2	2 3	1 1	3 2	1 1	2 2	2 2	3 3	2 2	2 2	2 3
CNG003																					
D8S1751																					
D8S1836																					
CNG004																					
CNG005	4 4	2 4	4 4	2 2	4 4	4 4	4 4	4 4	4 4	1 4	2 2	2 2	2 2	2 2	2 2	4 4	2 4	4 4	2 2	2 4	2 2
D8S2334	9 9	7 9	7 3	7 7	7 3	3 3	1 1	9 9	2 2	4 3	5 5	9 9	9 9	9 9	9 9	1 1	9 1	2 2	9 9	9 3	9 8
D8S1926	2 2	4 2	5 4	2 2	3 4	4 4	5 5	2 2	5 5	4 4	2 2	2 2	2 2	2 2	2 2	2 2	4 2	2 2	1 1	1 5	1 2
D8S1925	4 4	4 4	1 4	5 5	6 7	4 4	6 6	4 4	6 6	3 4	6 6	6 6	6 6	6 6	6 6	6 6	7 4	6 6	6 6	6 4	6 6
Mutation	82delT C28→32X										Altered Splicing 178+1g→a							C286T R96X			

Figure 1. MDM disease-associated haplotypes for microsatellite markers in the 8qter region. The marker order is from centromere to telomere. The shaded area represents the interval defined by disequilibrium analysis. There are three ancestral haplotypes corresponding to three different mutations. A, patients from Algeria; C, patients from Croatia.

Table 1. Sequences of new developed primers

Name	Number of alleles	Forward sequences (5'→3')	Reverse sequences (5'→3')
CNG001	11	CACTGAAGTCTCACTGGAG	GAAACTTTACCTCACTGAATTT
CNG002	4	CATCCTGCAGAAGGAAAGTA	CTTCTAGGAAGTCAAGCGTG
CNG003	13	CTGGAGGAATTGTGCTCAG	CCTCTGTCTGAGGCCTGT
CNG004	11	GTCTCTGTTGTGGGGTGA	AGGGTGGAGAGCAGAGAC
CNG005	5	CCATTTAGAACCAATTCTCT	GCTGTTGAGCAACAATCTCT

cousin marriages and one from an uncle/niece marriage); in five families no consanguinity loop was found.

Linkage studies

Genotyping in the 8qter interval was performed using eight markers from public databases and five new markers which we developed (Table 1). All the patients showed a homozygous region for markers at 8qter, even when they were not known to be consanguineous (Fig. 1). The maximum LOD score was 24.19 for the marker *CNG003* at $\theta = 0.0$. Recombination events and loss of homozygosity reduced the smallest cosegregating interval to 1 cM, containing three microsatellite markers: *CNG003*, *D8S1751* and *D8S1836*. Flanking markers were *CNG002* and *CNG004*, based on recombination events observed in families 1, 14, 17 and 19 for the centromeric part and in families 1 and 5 for the telomere. Markers mapping within the interval defined by recombination events showed, as expected, strong and significant allelic association with MDM ($P_{\text{excess}} = 0.70, 0.68$ and 0.63 at *CNG003*, *D8S1751* and *D8S1836*, respectively; $\chi^2 < 0.0001$) (Fig. 1). Three ancestral haplotypes were observed; the first (3-3-2) was found in nine large Algerian and four Croatian kindreds. A second haplotype (7-1-5) was observed in three Algerian families and, finally, a third haplotype (8-1-4) was present in three Croatian families (Fig. 1).

Physical map and identification of candidate genes

We constructed a partial physical map consisting of five neighboring contigs: centromere- 18393, 19078, 15579 (partly) // 16892 // 16007 -telomere, which was in agreement with recent data from 'Golden Path' (<http://genome.ucsc.edu/>). Two markers (*CNG003* and *D8S1751*) showing significant linkage disequilibrium were contained in contig 16892, whereas the third marker (*D8S1836*) was not found in any of the identified contigs. The contig 16892 includes six overlapping sequences, spanning about 300 kb: AC073385, AB000381, AC011976, AC015718, AF176678 and AF235094. They were compared with the annotated sequences of databases such as Ensembl for their gene content. Contig 16892 contains a cluster of Ly-6 homologous human genes, including *E48* (Ly-6D-pending) (7), *GML* (8) or glycosylphosphatidylinositol (GPI)-anchored molecule-like protein (Ly-6DL, MIM 602370), *ARS* (5) and prostate stem cell antigen (*PSCA*) (9). All of them are members of the Ly-6/uPAR family of receptor and secreted proteins. The Ly-6 proteins were initially identified as mouse lymphocyte antigens; uPAR is the urokinase-type plasminogen activator receptor. This family is defined by a highly conserved pattern of disulfide bridges (10,11) and a gene structure which usually contains four exons, the first of which is untranslated.

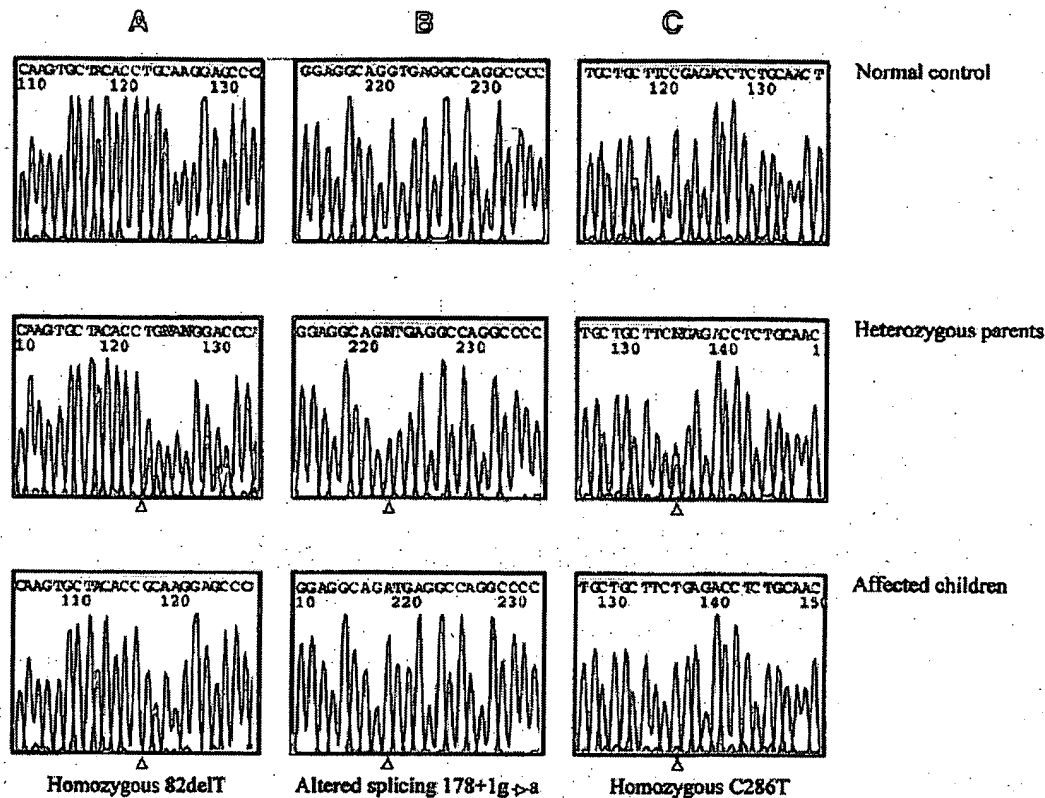


Figure 2. *ARS (component B)* mutations in MDM patients. A homozygous deletion (A) in nucleotide 82 leading to a frameshift and a premature stop codon is associated with the first haplotype (Fig. 1). The second haplotype (B) is associated with a splice site mutation, and the third (C) with a point mutation (C286T), which changes arginine at position 96 to a stop codon. Arrowheads indicate the positions of the mutations. Parents were heterozygous in all cases.

Mutation analysis

The *E48* gene is known to be expressed in human keratinocytes, but not in lymphocytes (12) and has been demonstrated to be involved in the desmosomal cell-cell adhesion of keratinocytes (13), making it a candidate gene for PPK. *E48* was shown to contain only three exons (12). Immunofluorescence analysis in patient skin with an antibody directed against *E48* demonstrated a normal expression pattern (data not shown), suggesting that this gene is not the MDM gene. This finding was further supported by sequence analysis showing no mutations in the three coding exons of the *E48* gene. Sequencing of the three coding exons of the *GML* gene, which is induced by the p53 tumor suppressor and shares a similar genomic organization with the other genes of the *Ly-6* family (8), also failed to reveal mutations. The *ARS (component B)* gene is also predicted to contain three exons, and to encode a protein of 103 amino acids, but since the genomic sequence is only available in GenBank, the existence of a first untranslated exon cannot be completely excluded. Mutation analysis of the three exons of the *ARS (component B)* gene in our 19 families revealed three different homozygous mutations corresponding to the three different ancestral haplotypes. The first haplotype was observed in patients from 13 families of Algerian and/or Croatian origin (Fig. 1), in which we found a single nucleotide deletion (82delT) leading to a frameshift (Fig. 2) and creation of a premature stop codon at amino acid position 32. A splice

site mutation affecting the invariant G of the donor splice site GT dinucleotide in the second intron was found in three Algerian families, which exhibit the second haplotype. This mutation is expected to lead to aberrant splicing. Three Croatian families showed a point mutation at position 286 (C286T), which changes arginine at position 96 to a stop codon, and which corresponds to the third haplotype (Fig. 2). Although this mutation is at the end of the protein, the truncated version of the protein lacks a cysteine implicated in one of the highly conserved disulfide bridges.

Expression analysis

Expression of SLURP-1 transcripts was investigated in cultured keratinocytes and tissue samples from normal and affected individuals. Northern blot analysis (Fig. 3A) showed strong expression of SLURP-1 mRNA in cultured keratinocytes derived from a plantar skin biopsy from a normal control subject, but absence of expression in keratinocytes from the involved plantar skin of patients. It was not detected in cultured keratinocytes from normal trunk skin or in biopsies from control trunk epidermis. On the other hand, RT-PCR analysis, which is more sensitive (Fig. 3B), revealed SLURP-1 mRNA in cultured keratinocytes from skin biopsies from different body sites in both controls and MDM patients. In biopsies from normal subjects, SLURP-1 mRNA was found to be expressed in epidermis, foreskin, scalp skin and fetal

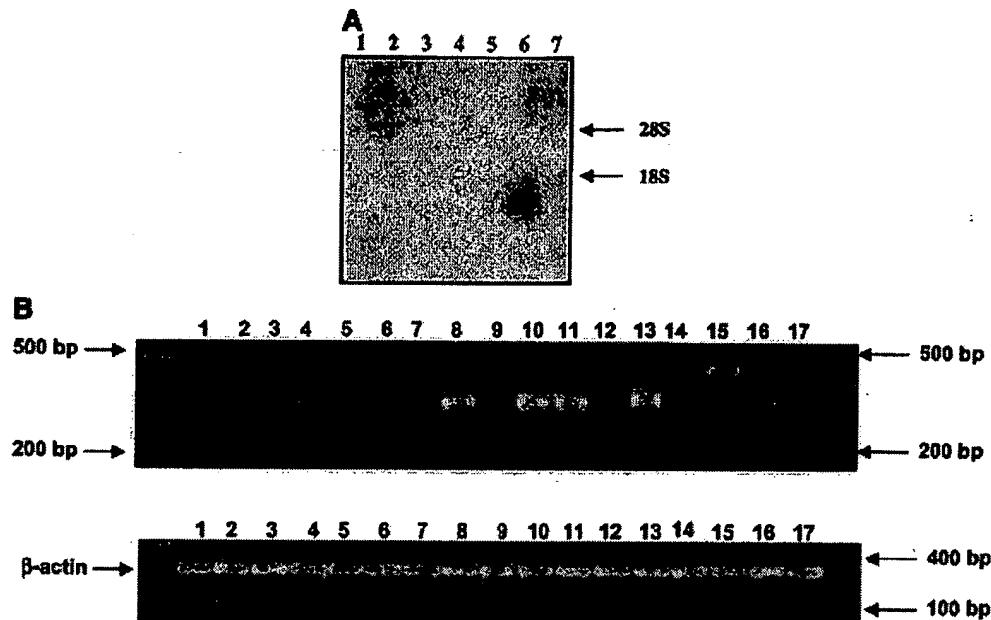


Figure 3. (A) Expression of SLURP-1 mRNA. Northern blot hybridization of RNA from cultured keratinocytes and skin biopsies with a SLURP-1 probe (nucleotides 1852–1991 from GenBank accession no. X99977). SLURP-1 is strongly expressed in cultured keratinocytes derived from a control plantar skin biopsy (lane 6) but is absent in biopsies from patients (lanes 1–3) and in keratinocytes from normal trunk skin controls (lanes 4 and 5). Similarly, no SLURP-1 mRNA could be detected in biopsies from normal trunk skin from controls (lane 7). These results indicate that SLURP-1 is mainly expressed in plantar, and most likely in palmar skin, which are the principal sites of MDM lesions. (B) Expression analysis of the SLURP-1 transcript by RT-PCR. (Top) RT-PCR of SLURP-1 specific primers in various tissues (lanes 1–11) and cultured cells (lanes 12–17). (Bottom) RT-PCR with β -actin primers as control. Lane 1, fetal brain; lane 2, adult liver; lane 3, adult lung; lane 4, fetal bladder; lane 5, adult kidney; lane 6, adult colon; lane 7, adult uterus; lane 8, epidermis; lane 9, scalp skin; lane 10, inner leaflet of human foreskin; lane 11, outer leaflet of human foreskin; lane 12, human fibroblast; lane 13, keratinocytes from plantar skin; lane 14, keratinocytes from trunk; lanes 15–17, keratinocytes from plantar skin of patients 4, 17, 13, 3 and 1, 9, respectively.

bladder, but not in the other tissues tested (Fig. 3B). Interestingly, in a patient with a splice site mutation we found two RT-PCR products with different sizes compared with controls, indicating that no normal mRNA is formed in this patient. These results indicate that SLURP-1 is mainly expressed in plantar, and most likely, in palmar skin, which corresponds to the sites of MDM lesions.

DISCUSSION

This is the first time that a secreted protein has been implicated in a PPK. The Ly-6/uPAR superfamily of proteins was initially identified in mice. The Ly-6 locus encodes at least seven structurally related proteins clustered on murine chromosome 15. On the basis of synteny, it has been suggested that the human homologs reside on human chromosome 8q, distal to *Myc-1*, with the exception of protectin (*CD59*) which is located on 11p13 (14). Attempts to isolate the human homologs through interspecies homology have been hampered by an apparently rapid divergence of genes between species. The superfamily has been classified into two subfamilies (5), the first of which includes GPI-anchored receptor proteins with 10 conserved cysteine residues such as retinoic acid-induced gene E (*RIG-E*) (15), the *E48* antigen (7), the *PSCA* (9), *CD59* or protectin (14) and uPAR. The ligands for the Ly-6-related human *CD59* and uPAR are known and contain EGF-like repeats (6). Similarly, the first ligand described for a mouse Ly-6 protein (Ly-6D or ThB, the murine homolog for *E48*) was recently identified as a small 9 kDa protein with significant homology to the EGF-repeats

of the Notch family (16). The second subfamily, characterized by lack of a GPI-anchoring signal sequence and at least eight of the 10 conserved cysteines, includes secreted snake and frog cytotoxins and the recently described SLURP-1 protein, which is the first secreted mammalian member of the Ly-6/uPAR superfamily to be reported. SLURP-1 was isolated from peptide libraries prepared from an ultrafiltrate of human blood and from urine (5). Its function is unknown at present but phylogenetic analysis has shown that it is more closely related to the snake cytotoxins than to the mammalian GPI-anchored receptors (5). Therefore, SLURP-1 is likely to function as a ligand for a receptor yet to be identified. As a secreted molecule it may compete with members of the GPI-anchored receptor Ly-6 subfamily for binding to ligands (e.g. urokinase-type plasminogen activator) or to other molecules containing EGF-repeats including Notch, which are similar to the processed Notch-ligand delta (17). Finally, SLURP-1 may interfere with weak intercellular adhesion, as has been shown for Ly-6D and Ly-6DL (16). The discovery of SLURP-1 as the cause of a PPK of the Meleda type implicates yet another type of protein in the development of PPKs.

MATERIALS AND METHODS

Human material

Three dermatologists (B.B., D.H. and A.B.-K.) recorded clinical data, pedigree information and performed skin biopsies for

Table 2. Primer sequences for ARS, E48 and GML

Name	Forward sequences (5'→3')	Reverse sequences (5'→3')
ARS-ex1	GAACAGTGAGTTCCCCAGTG	CACTGAGAATGAGGAGGGTG
ARS-ex2	GATGTCAGCGAGACTCCTTC	CAGGACTGGGTCTCTGAGG
ARS-ex3	GAACAGGGATCACAGGGAG	GTCATGTCCACTCTTGGCTT
E48-ex1	CACAGCAGCAGGAACAGCAG	TCGTCAGCTCCAGGCTCCTAGT
E48-ex2-3	CAGGCCCTGCTAAGTCACCA	TCCCCAGAGAAAGGGAAGGA
GML-ex2	GCAGAGTCAGGGAGACTCAT	CCACCCCTGATTACACAGAC
GML-ex3	TGTGCAGGCTAGGAGAAGTC	GAGTACCTGGCTCCACAAGA
GML-ex4	CACAGCGTGGGAGTGTAGAA	CCATAAATGGGCCACCTAGA

histological examination (18). Blood samples were collected from each participant family member and skin biopsies were obtained from most of the patients after obtaining written informed consent. DNA extraction from peripheral blood leukocytes was performed using standard procedures.

Genetic analysis

Genotyping with fluorescent markers was carried out as described previously (4). Haplotypes were constructed assuming the most parsimonious linkage phase. Linkage programs were used on the assumption of autosomal recessive inheritance, full penetrance and a disease frequency of 1 in 100 000 in the general population. Pairwise LOD scores were calculated with the MLINK program of the LINKAGE 5.1 package (19), incorporating consanguineous loops into the pedigree files if the information about consanguinity was given by the patients. For linkage disequilibrium analysis, we examined the frequencies of each allele in the affected and the normal chromosome population to define the presumed ancestral haplotype. Chromosomes shared by two siblings or homozygous were counted only once. The excess of the disease-associated alleles was calculated using the P_{excess} equation (20): $P_{\text{excess}} = (P_{\text{affected}} - P_{\text{normal}}) / (1 - P_{\text{normal}})$, in which P_{affected} and P_{normal} denote the frequency of the disease-associated allele on disease-bearing (34 chromosomes) and normal chromosomes (40 chromosomes), respectively. For χ^2 estimation, we used the combined-allele method (21). The significance level ($\alpha = 0.05$) was corrected using Bonferroni's procedure (22) as follows: $\alpha' = 1 - (1 - \alpha)^{1/L}$, where L is the number of individual tests (13 tests in our study) and was 0.003.

Construction of a physical contig map

The sequences from the interval between the marker *D8S1717* and the telomere were identified by the Genoscope working draft utility (<http://www.genoscope.cns.fr/cgi-bin/WD.cgi>). Based on the Human Gene Map (<http://www.ncbi.nlm.nih.gov/genemap>), this tool identified working draft sequences which contained one or more RHdb markers from the interval by e-PCR. These genomic sequences include cosmids, P1-derived artificial chromosome (PAC) and bacterial artificial chromosome (BAC) clones, most of which were unfinished sequences (phase 0–1). To construct a physical contig map of the region, we performed a search for BAC end sequences in the TIGR database with these working draft

sequences. We identified additional BAC clones, which we analyzed on the human fingerprint contig map of the Washington University Genome Center, which permitted assembly of clones and contigs in a physical order. A strategy of extension and junction formation between contigs was followed, using the Sequence Tag Connectors approach. The resulting partial physical map of our interval consisted of five clone contigs containing about three quarters of the RHdb markers from the gene map interval. The two flanking contigs could be excluded due to their content of markers which showed recombination events in affected individuals. Ten new (CA)_n repeat microsatellites from sequences of the three remaining contigs were developed (Table 1), but only five of them were polymorphic and useful for linkage analysis. Sequences from the three contigs were compared with databases such as the Ensembl genome server (<http://www.ensembl.org>), where results of new and already known gene structures were annotated by several gene prediction programs, in order to identify candidate genes for mutation analysis.

Mutation screening

Mutation analysis was performed in affected patients and in both parents in the 19 families, and in supplementary non-affected siblings in cases of missing parents. We designed intronic oligonucleotide primers for *ARS*, *E48* and *GML* flanking the coding exons (Table 2) using the Primer3 program from the genomic sequences X99977, X82693 and AB000381, respectively. The PCR reaction was performed in a 50 μ l volume containing 100 ng of genomic DNA (in 10 μ l) using standard procedures (23). After an initial denaturation step at 96°C for 5 min, Taq polymerase was added at 94°C (hot start) and 35 cycles of amplification were performed consisting of 30 s at 94°C, 40 s at the optimal annealing temperature (58°C) followed by a 10 min terminal elongation step. Purified PCR products (1–1.5 μ l) were added to 1 μ l of sense or antisense primer (10 μ M) and 3 μ l of BigDye terminator mix (PE Applied Biosystems). The linear amplification consisted of an initial denaturation step at 96°C, 25 cycles of 10 s of denaturation at 96°C, a 5 s annealing step (55–61°C) and a 4 min extension step at 60°C. The reaction products were purified and sequenced on an Applied Biosystem Sequencer 3700. Both strands from all patients and controls were sequenced for the entire coding region and the intron/exon boundaries.

Immunofluorescence analysis

Frozen skin from patients and control individuals was incubated with a monoclonal antibody (mAb E48) (7) directed against E48 at a 1:100 dilution. Antibodies were then visualized by sequential incubation with biotinylated horse anti-mouse IgG (Vector Laboratories) at a dilution of 1:100 and TexasRed Streptavidin (Gibco BRL) at a dilution of 1:400.

RNA isolation, northern blot analysis and RT-PCR

RNA isolation from cultured keratinocytes and skin biopsies was carried out as previously described (24). We generated specific PCR probes for the 3'UTR of *ARS* (nucleotides 1852–1991 of X99977). After purification using the QIAquick PCR purification kit (Qiagen), these probes were radiolabeled with ³²P and exposed to Kodak film for 3 days at –80°C. The SLURP1-specific probes were hybridized to human keratinocyte total RNA (13 µg) from different skin areas (plantar skin of patients, normal controls and trunk epidermis from controls). RT-PCR was performed using the OneStep RT-PCR kit (Qiagen) with the forward primer from exon 1 (nucleotides 572–592) and reverse primers (nucleotides 1817–1797) from exon 3. The RT-PCR conditions were 50°C for 30 min for reverse transcription, incubation at 95°C for 15 min for inactivation of reverse transcriptases, followed by 35 cycles of 94°C for 1 min, 60°C for 30 s and 72°C for 50 s, and final extension for 10 min at 72°C. RT-PCR fragments were run on 1% agarose gel and visualized under an ultraviolet transilluminator.

GenBank and SwissProt accession numbers

ARS (component B) gene, X99977; SLURP-1, P55000; *E48*, X82693; and *GML*, AB000381.

ACKNOWLEDGEMENTS

We wish to thank the family members for their participation and we would like to acknowledge the technical support of the Généthon DNA bank. We are especially grateful to Susan Cure for help in writing this manuscript. This study was supported by the Centre National de Génotypage (CNG), Association Française contre les Myopathies (AFM) and Généthon. D.H. was supported by the Swiss National Foundation.

REFERENCES

- Kelsell, D.P. and Stevens, H.P. (1999) The palmoplantar keratodermas: much more than palms and soles. *Mol. Med. Today*, **5**, 107–113.
- Toomes, C., James, J., Wood, A.J., Wu, C.L., McCormick, D., Lench, N., Hewitt, C., Moynihan, L., Roberts, E., Woods, C.G. *et al.* (1999) Loss-of-function mutations in the cathepsin C gene result in periodontal disease and palmoplantar keratosis. *Nature Genet.*, **23**, 421–424.
- Norgett, E.E., Hattrell, S.J., Carvajal-Huerta, L., Ruiz Cabezas, J.C., Common, J., Purkis, P.E., Whitlock, N., Leigh, I.M., Stevens, H.P. and Kelsell, D.P. (2000) Recessive mutation in desmoplakin disrupts desmoplakin-intermediate filament interactions and causes dilated cardiomyopathy, woolly hair and keratoderma. *Hum. Mol. Genet.*, **9**, 2761–2766.
- Fischer, J., Bouadjar, B., Heilig, R., Fizames, C., Prud'homme, J.F. and Weissenbach, J. (1998) Genetic linkage of Meleda disease to chromosome 8qter. *Eur. J. Hum. Genet.*, **6**, 542–547.
- Adermann, K., Wattler, F., Watter, S., Heine, G., Meyer, M., Forssmann, W.G. and Nehls, M. (1999) Structural and phylogenetic characterization of human SLURP-1, the first secreted mammalian member of the Ly6/uPAR protein superfamily. *Protein Sci.*, **8**, 810–819.
- Gumley, T.P., McKenzie, I.F.C. and Sandrin, M.S. (1995) Tissue expression, structure and function of the murine Ly-6 family of molecules. *Immunol. Cell Biol.*, **73**, 277–296.
- Brakenhoff, R.H., Gerretsen, M., Knippels, E.M.C., van Dijk, M., van Essen, H., Weghuis, D.O., Sinke, R.J., Snow, G.B. and van Dongen, G.A.M.S. (1995) The human E48 antigen, highly homologous with the murine Ly-6 antigen ThB, is a GPI-anchored molecule apparently involved in keratinocyte cell-cell adhesion. *J. Cell Biol.*, **129**, 1677–1689.
- Kimura, Y., Furuhashi, T., Urano, T., Hirata, K., Nakamura, Y. and Tokino, T. (1997) Genomic structure and chromosomal localization of GML (GPI-anchored molecule-like protein), a gene induced by p53. *Genomics*, **41**, 477–480.
- Reiter, R.E., Gu, Z., Watabe, T., Thomas, G., Szegedi, K., Davis, E., Wahl, M., Nisitani, S., Yamashiro, J., Le Beau, M.M. *et al.* (1998) Prostate stem cell antigen: a cell surface marker overexpressed in prostate cancer. *Proc. Natl Acad. Sci. USA*, **95**, 1735–1740.
- Ploug, M., Kjalke, M., Ronne, E., Weidle, U., Hoyer-Hansen, G. and Dano, K. (1993) Localisation of the disulfide bonds in the NH2-terminal domain of the cellular receptor for human urokinase-type plasminogen activator. A domain structure belonging to a novel superfamily of glycolipid-anchored membrane proteins. *J. Biol. Chem.*, **268**, 17539–17546.
- Fletcher, C.M., Harrison, R.A., Lachmann, P.J. and Neuhaus, D. (1993) Sequence-specific 1H-NMR assignments and folding topology of human CD59. *Protein Sci.*, **12**, 2015–2027.
- Brakenhoff, R.H., van Dijk, M., Knippels, E.M.C. and Snow, G.B. (1997) A gain of novel tissue specificity in the human Ly-6 gene E48. *J. Immunol.*, **159**, 4879–4886.
- Schrijvers, A.H.G.J., Gerretsen, M., Fritz, J.M., van Walsum, M., Quak, J.J., Snow, G.B. and van Dongen, G.A. (1991) Evidence for a role of monoclonal antibody E48 defined antigen in cell-cell adhesion in squamous epithelia and head and neck squamous cell carcinoma. *Exp. Cell Res.*, **196**, 264–269.
- Bickmore, W.A., Longbottom, D., Oghene, K., Fletcher, J.M. and van Heyningen, V. (1993) Colocalization of the human CD59 gene to 11p13 with the MIC11 cell surface antigen. *Genomics*, **17**, 129–135.
- Mao, M., Yu, M., Tong, J.H., Ye, J., Zhu, J., Huang, O.H., Fu, G., Yu, L., Zhao, S.Y., Waxman, S. *et al.* (1996) RIG-E, a human homolog of the murine Ly-6 family, is induced by retinoic acid during the differentiation of acute promyelocytic leukemia cells. *Proc. Natl Acad. Sci. USA*, **93**, 5910–5914.
- Apostolopoulos, J., McKenzie, I.F.C. and Sandrin, M.S. (2000) Ly6d-L, a cell surface ligand for mouse Ly6d. *Immunity*, **12**, 223–232.
- Qi, H., Rand, M.D., Wu, X., Sestan, N., Wang, W., Rakic, P., Xu, T. and Artavanis-Tsakonas, S. (1999) Processing of the Notch ligand delta by the metalloprotease Kuzbanian. *Science*, **283**, 91–94.
- Bouadjar, B., Benmazouz, S., Prud'homme, J.F., Cure, S. and Fischer, J. (2000) Clinical and genetic studies of 3 large, consanguineous, Algerian families with mal de Meleda. *Arch. Dermatol.*, **136**, 1247–1252.
- Lathrop, G.M., Lalouel, J.M., Julier, C. and Ott, J. (1985) Multilocus linkage analysis in humans: detection and estimation of recombination. *Am. J. Hum. Genet.*, **37**, 482–498.
- Hästbacka, J., de la Chapelle, A., Mahtani, M.M., Clines, G., Reeve-Daly, M.P., Daly, M., Hamilton, B.A., Kusumi, K., Trivedi, B., Weaver, A. *et al.* (1994) The diastrophic dysplasia gene encodes a novel sulfate transporter: positional cloning by fine-structure linkage disequilibrium mapping. *Cell*, **78**, 1073–1087.
- Aksentijevich, I., Pras, E., Gruberg, L., Shen, Y., Holman, K., Helling, S., Prosen, L., Sutherland, G.R., Richards, R.I., Dean, M. *et al.* (1993) Familial Mediterranean fever (FMF) in Moroccan jews: demonstration of a founder effect by extended haplotype analysis. *Am. J. Hum. Genet.*, **53**, 644–651.
- Weir, B.S. (1990) *Genetic Data Analysis*. Sinauer, Sunderland, MA.
- Vignal, A., Gyapay, G., Hazan, J., Nguyen, S., Dupraz, C., Cheron, N., Becuwe, N., Tranchant, M. and Weissenbach, J. (1993) Nonradioactive multiplex procedure for genotyping of microsatellite markers. In Adolph, K.W. (ed.), *Gene and Chromosome Analysis. Part A*, Vol. 1. Academic Press, San Diego, pp. 211–221.
- Huber, M., Yee, V.C., Burri, N., Vikerfors, E., Lavrijsen, A.P., Paller, A.S. and Hohl, D. (1997) Consequences of seven novel mutations on the expression and structure of keratinocyte transglutaminase. *J. Biol. Chem.*, **272**, 21018–21026.